Robust Energy Management Strategy based on the Battery Fault Management for Hydraulic-electric Hybrid Vehicle

Elkhatib Kamal and Lounis Adouane

Institut Pascal/IMobS3, UCA/SIGMA UMR CNRS 6602, Clermont-Ferrand, France

Abstract: This paper deals with a robust energy management strategy, including a battery fault detection and compensation for a hydraulic-electric hybrid vehicle. The overall control and management strategy aims to minimize total energy consumption while ensuring a better battery life. Many power management strategies do not consider battery faults which could accelerate battery aging, decreasing thus its life and could cause also thermal runaway, which may cause fire and battery explosions. Therefore, battery fault tolerant control to guarantee the battery performance is also proposed in this paper. The proposed strategy consists of fuzzy supervisory fault management at the highest level (the second). This level is responsible to detect and compensate the battery faults, generating optimal mode and healthy state of charge set point for first level to prevent overcharge or/and over-discharge. In the first level, an energy management strategy is developed based on neural fuzzy strategy to manage power distribution between electric motor and engine. Then, there are robust fuzzy controllers to regulate the set points of each vehicle subsystems to reach the best operational performance. The Truck-Maker/MATLAB simulation results confirm that the proposed architecture can satisfy power requirement for any unknown driving cycles and compensate battery faults effect.

1 INTRODUCTION

Growing environmental concerns coupled to the decreasing of fossil fuel energy sources stimulate highly research on new vehicle technologies. Electric vehicles (EVs) and Hybrid Electric Vehicles (HEV) appear to be one of the most promising technologies for reducing fuel consumption and pollutant emissions (Panday and Bansal, 2016). Energy management in vehicles is an important issue because it can significantly influence the performances of the vehicles. Several methods for energy management and optimization aiming at the minimization of different cost functions have been published, such as dynamic programming (Abdrakhmanov and Adouane, 2017), (Tate et al., 2010), the equivalent consumption minimization strategy (Tulpule et al., 2010), Pontryagin's Minimum Principle (PMP), (Hou et al., 2014) and genetic algorithm (Martnez et al., 2016). Therefore, there are nowadays different blending levels of pure EV and Hybrid Electric Vehicle (HEV) available on the current automobile market. According to the blending level, various size, type and number of battery cells are mounted in HEVs and EVs (Lu et al.,

2013). Unlike conventional fuel, battery cells as an energy source have stricter requirement on working environment (Striebel et al., 2005). Many approaches to power management strategy of hybrid vehicle do not consider the effect of control strategy on the faulty battery (Tulpule et al., 2010), (Martnez et al., 2016), (Kamal et al., 2017b), (Kamal et al., 2017a). It is known that, Lithium-ion batteries are considered as the most promising energy storage device in HEV, due to their inherent benefits of high power and energy density, long lifespan and low maintenance cost. These growing demands make the battery performance and life of critical importance. Although Lithium-ion batteries are known as long-service devices, their lives depend greatly on environmental condition and operation mode (Maleki and Howard, 2006). Environmental conditions such as overcharging, overdischarging and the temperature will shorten service life. In addition, the sensors in the battery system may present different kinds of failures due to high temperature, overcharging/overdischarging and battery design and or vibrations (Xing et al., 2013). If the current or voltage sensor is faulty, the battery State of Charge (SOC) estimations may be affected,

this may result in the battery suffering from over-charge or/and over-discharge (Plett, 2004). This will accelerate the battery aging, decrease the battery life and cause thermal runaway, which in the worst cases may cause fire and battery explosions and then the fire and the vehicle destruction. Therefore, a reliable battery sensor and actuator fault tolerant control to guarantee the battery performance, safety and life while simultaneously minimizing the total energy consumption (summation of electric battery and fuel) of Hydraulic-Electric Hybrid Vehicle (HHEVs) are addressed in this paper. Robust Energy Management Strategy (REMS) is proposed based on neural networking, fuzzy logic, fuzzy observer and rule based optimization. The REMS has been realized based on the analysis results of the energy management strategy presented in (Kamal et al., 2017a). An Intelligent Supervisory Switching Mode and Battery Management Controller (ISSMBMC) based on fuzzy logic, fuzzy observer and rule based optimization is developed in the second level (the highest level) that is capable of managing all of the possible bus operation modes, compensate the battery faults, generating optimal mode and SOC set points for first level. The proposed algorithm in this level based on fuzzy observer to estimate the faults is then investigated for the detection, isolation and compensation of sensor (voltage sensor) and actuator (current sensor) battery faults. A Takagi-Sugeno's (TS) fuzzy model is adopted for fuzzy modeling of the system and establishing fuzzy state observers. The concept of Parallel Distributed Compensation (PDC) (Kamal et al., 2017b) is employed to design fuzzy control and fuzzy observers from the TS fuzzy models. Sufficient conditions are derived for robust stabilization in the sense of Lyapunov stability, for sensor faults, actuator faults and state variables unavailable for measurements. The sufficient conditions are formulated in the format of Linear Matrix Inequalities (LMI). The energy management strategy in the first level is formulated based on neural fuzzy strategy for minimizing the total energy consumption while meeting the driver power demand. This level decides the optimal combination of power sharing between different energy sources (battery and Internal Combustion Engine (ICE)) to maximize overall vehicle efficiency. In addition, there are adaptive fuzzy controller based on (Hamed and Almobaied, 2011) which are used to track the set points of Electric Motor (EM) and Hydraulic Motor (HM) via the ICE, in order to reach peak performance and acceptable operation indexes while taking into consideration the dynamic behavior of EM, ICE and HM. The proposed strategy can be used for both offline and online scenarios. Since this paper makes more

the focus on the second Level 2, only while the first level is designed based on (Kamal et al., 2017a). The proposed strategies, implemented in simulation using TruckMaker software, confirm that the proposed architecture can satisfy the power requirement for any unknown driving cycles and compensate the effect of the battery faults. The results of this paper support that the proposed strategy is capable of: (i) detection, isolation and compensation the battery voltage sensor fault and battery currant actuator fault; (ii) minimizing the total energy consumption; (iii) being implemented in real-time; (iv) it does not require beforehand a-priori knowledge of the driving event; (v) reducing the number of rules needed in fuzzy control; (vi) maintaining the ICE near its optimal operating range; (vii) keeping SOC within the range which promotes battery longevity.

In addition to the main objectives in this paper, an accurate and reliable model of the studied hybrid vehicle is also highlighted in Section 2. The studied vehicle is a hybrid bus, based on a series-parallel power-split hybrid architecture. This hybrid bus is called BUSINOVA and is developed by SAFRA company (cf. Figures 1 and 2).

The paper is organized as follows. The overall HHEV description and modeling is given in section 2. In section 3, the proposed robust energy management Strategy structure is developed. Section 4 shows the experiment model validation and fault effects analysis. Section 5 is devoted to give a conclusion and some prospects.

2 OVERALL HHEV MODELING AND DESCRIPTION

In order to study and develop an efficient energy management strategy including the battery fault management for HHEVs, an accurate and reliable model is needed. Therefore, this section will make a focus on the modelling and analysis of the studied HHEV with its different operations modes. Truck-Maker/MATLAB software is used to simulate precisely the studied hybrid vehicle.

2.1 HHEV Description and Modelling

The studied vehicle corresponds to BUSINOVA bus shown in Figure 1. This bus has three actuations: electric, hydraulic and thermal. The principle source of the propulsion in the vehicle is an EM which may be supplemented by the HM via ICE. The hydraulic system block consists of variable-displacement of

HM, and an ICE driven fixed-displacement of Hydraulic Pump (HP). The ICE is directly connected to a fixed displacement pump, which converts engine mechanical power into hydraulic power as shown in the vehicle configuration and power flow diagram (cf. Figure 2). The BUSINOVA is equipped with electric, hydrostatic and dissipative braking capabilities. The dissipative brake is a mechanical brake which dissipates energy as heat through friction. Electric and hydrostatic brakes are linked to the hydraulic motor in a regenerative braking system that is capable of recovering a portion of the kinetic energy of braking that would otherwise be dissipated. An Electrical Junction (EJ) exists between the battery, accessories (Access) and dual converter as well as a Mechanical Junction (MJ) between the HM and EM.

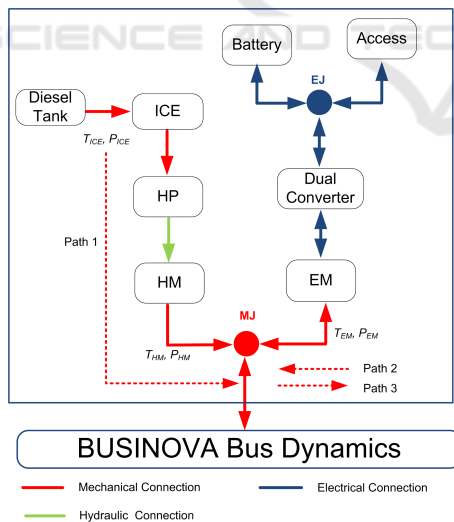Figure 1: BUSINOVA a Hydraulic-Electric Hybrid bus.

Figure 2: BUSINOVA bus configuration and power flow. T_{ICE}, T_{HM}, T_{EM} and P_{ICE}, P_{HM}, P_{EM} are the produced torque and power for the ICE, HM and EM, respectively.

2.2 Motoring Models

The BUSINOVA can operate according to the modes described below:

- The propulsion is fully supplied by EM (mode 1),
- The bus is actuated by the HM via ICE (mode 2),
- The mode 3 implies the hybrid operation of the EM and the HM via ICE,
- Recharge of the electric battery via ICE (mode 4),
- The regenerative braking (mode 5).

In this section, we will present the HM model through ICE and the EM models as the following.

2.2.1 Hydraulic Motor Coupled to Internal Combustion Engine

In this paper, ICE torque versus ICE speed is directly derived from the ICE fuel consumption model. The fuel flow rate $\dot{m}_f$ of the ICE is defined by

$$\dot{m}_f = f_{ICE}(T_{ICE}, \omega_{ICE}) \tag{1}$$

where ω_{ICE} is the ICE rotational speed. The function f_{ICE} is obtained from the ICE bench tests. The power consumed by the ICE (P_{ICE}) is given by $P_{ICE} = \dot{m}_f(T_{ICE}, \omega_{ICE})Q$, (i.e., P_{ICE} is the instantaneous power of the fuel expressed in terms of $\dot{m}_f$ and the lower heating value of the fuel ($Q = 43\text{MJ/kg}$)).

2.2.2 Electric Motor

The studied hybrid bus uses a 103 KW permanent magnet synchronous machine as EM. The powers required for the EM were calculated from the known EM torque and speed by using EM efficiency curve. The output torque T_{EM} of the EM is defined by

$$T_{EM} = f_{EM}(P_{EM}, \omega_{EM}) \tag{2}$$

where P_{EM} is the EM input power, ω_{EM} is the EM current speed. The function f_{EM} is also obtained from the EM bench test. The EM can operate in motor or generator mode.

2.3 BUSINOVA Battery Modeling

One of the most important is the SOC for the battery fault management strategy, since during the operation of the battery, the SOC cannot be measured directly. Therefore the estimation of the SOC is needed. To obtain a reliable SOC estimation, an accurate model of the battery is needed. Different Lithium-ion battery models are developed in the literature for various purposes. The equivalent electrical circuit models and the electrochemical models are the most widely used in EV studies. The electrical circuit models use equivalent electrical circuits to show current-voltage characteristics of batteries by using voltage and current sources, capacitors, and resistors. For BUSINOVA

bus battery model, we select the model presented in (Sepasi et al., 2014) as a reference model (cf. Figure 3). The selected battery model consists of two parts of the Energy Balance Circuit (EBC) and Voltage Response Circuit (VRS). The EBC delivers SOC to the VRS. To cover all BUSINOVA bus battery practical conditions, the model paramaters are considered to be a function of SOC, current, and temperature. Moreover to increase accuracy, this model has separate operating functions at low and high temperature for charging and discharging. Using Kirchoff's voltage law, the electrical behavior of the practical model can be expressed as follows:

$$V_{bat} = V_{oc} + I_{bat}R_o + V_1(t) + V_2(t) \qquad (3)$$

where V_{bat} is the battery terminal voltage, V_{oc} is the battery open circuit voltage (OCV), I_{bat} is the load current, t is the time varying, V_1, V_2 are the voltages across $R_1//C_1$ and $R_2//C_2$, where R_1, R_2 and C_1, C_2 are the RC branch resistors and capacitors, respectively, R_o is the internal resistance, which consists to the bulk resistance and surface layer impedance and T is the battery temperature. The dynamics of the nonlinear battery behavior can be characterized by the following equations,

$$\begin{aligned} \dot{x}(t) &= Ax(t) + Bu(t) \\ y(t) &= C(x)x(t) \end{aligned} \qquad (4)$$

Where $x(t) = \begin{bmatrix} V_1(t) \\ V_2(t) \\ SOC \end{bmatrix}$, $A = \begin{bmatrix} \frac{1}{R_1C_1} & 0 & 0 \\ 0 & \frac{1}{R_2C_2} & 0 \\ 0 & 0 & 0 \end{bmatrix}$,

$B = \begin{bmatrix} \frac{1}{C_1} \\ \frac{1}{C_2} \\ \frac{1}{C_n} \end{bmatrix}$, $C(x) = \begin{bmatrix} q_1(x) \\ 1 \\ q_2(x) \end{bmatrix}^T$, $u(t) = I_{bat}$ and $y(t) = V_{bat}$

where $q_1(x) = \frac{(I_{bat}R_o + V_1(t))}{V_1(t)}$ and $q_2(x) = \frac{V_{oc}}{SOC}$ are the nonlinear terms. Equation (4) indicates that the matrix $C(x)$ is not fixed, but change as functions of state variables, thus making the model to be nonlinear.
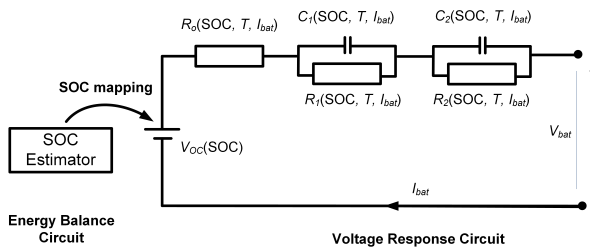

Figure 3: BUSINOVA Lithium-ion Battery equivalent electrical model.

3 PROPOSED ROBUST ENERGY MANAGEMENT STRATEGY (REMS)

After proposing an accurate model for the BUSINOVA bus, the aim of this section is to make the focus on the proposed REMS, embedded in the bus in order to minimize its total energy consumption while maximizing the global vehicle efficiency and compensate the battery faults. Therefore, in this section, an REMS structure is proposed which is capable of meeting various objectives including optimized power flow management, maintaining high operational efficiency of the ICE, and balancing EM and battery charge to maximize the global vehicle efficiency and detect and compensate the effect of the battery faults.

This proposed strategy consists of two control levels (cf. Figure 4). The second level has been developed by fuzzy strategy and fuzzy observer which decide which operating mode or combination of modes would be most efficient based on a healthy SOC (cf. section 3.1). This level consists of two blocks, the first block of this level is Battery Management Fuzzy Fault Tolerant Controller (BMFFTC) to detect and the compensate the battery faults and generate the healthy SOC for the Fuzzy Switching Mode Controller (FSMC) which selects the optimal mode for the second level. At the first level (cf. section 3.2), an energy management strategy has been developed for power splitting which decide the optimal combination of power sharing between different energy sources to maximize the overall vehicle efficiency. In addition, adaptive fuzzy controllers are used to track the set points of EM and HM via the ICE, in order to reach peak performance and acceptable operation indexes while taken in consideration of the dynamic behavior of EM, ICE and HM. In this paper, we will focus more on level 2 (cf. section 3.1), while the first level is designed based on (Kamal et al., 2017a).

3.1 Intelligent Supervisory Switching Mode and Battery Management Controller (Level 2: ISSMBMC)

The objective of this section is to optimize the selection mode and detect and compensate the battery sensor fault (battery terminal voltage sensor) and the actuator fault (battery input current actuator). This level is consists of BMFFTC and FSMC blocks to generate the selected mode and the SOC set point for the first level. Figure 5 shows the block diagram of the proposed level 2 block.
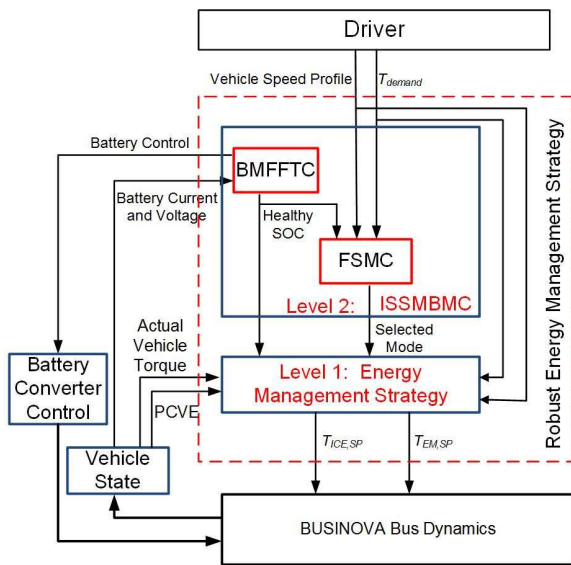
Figure 4: Developed REMS for BUSINOVA bus. In this figure the following acronyms are used: PCVE (Produced and Consumed Vehicle Energy); T_{demand} (Torque Demand) which is required to drive the vehicle and is defined by the global torque set point; $T_{ICE,SP}$ is the ICE torque set point and $T_{EM,SP}$ is the EM torque set point.

Figure 5: Schematic of the proposed level 2.

3.1.1 Fuzzy Switching Mode Controller (FSMC)

As mentioned in section 2.2, there are five modes of operations. In order to improve the studied HHEV operation, the proposed FSMC based on fuzzy logic and rule based, has to decide which operating mode (or combination of them) is appropriate. Many parameters (such as the value of SOC for the battery, required vehicle power, vehicle speed and maximum power supplied by the battery, etc.) must be considered to

choose the most efficient operation mode to manage and optimize the power flow. Based on the available output torque, the pedal position is converted into torque demand (T_{demand}). If $T_{demand} < 0$, the driver intends to decelerate the vehicle therefore regenerative braking mode is chosen. But, if $T_{demand} > 0$, the requiring torque is split between EM or/and HM via ICE. In the proposed algorithm, modes 1, 2, 3, and 4 are selected by fuzzy logic and mode 5 is selected by traditional logic. Fuzzy logic is well suited for selecting between modes 1, 2, 3 and 4, since the range or boundary is vague and not clearly specified due to the actual state of the vehicle (masse, velocity, etc.) for these modes. The ISSMBMC input variables are Vehicle Speed, T_{demand} and SOC, and its output variable is the operation mode (Mode). The fuzzy rule is constructed from 27 individual fuzzy rules. An example of the used rules is given for instance by this one: if T_{demand} is low and SOC is high and vehicle speed is high then Mode is model 1.

3.1.2 Battery Management Fuzzy Fault Tolerant Controller (BMFFTC)

The main objective for the BMFFTC is to mange and control the battery faults and generate the healthy SOC point for FSMC and the first level which affects the studied HHEV power optimization. This section presents a systematic fault diagnosis and control scheme for a battery cell to detect current and/or voltage sensor faults, and compensate its effect. For the diagnostic and control scheme implementation, new Fuzzy Fault Tolerant Control (FFTC) based on fuzzy adaptive observer is proposed. The algorithm based on mechanism is used to estimate the faults then investigated for detection, isolation and accommodation of the battery sensor fault (battery terminal voltage sensor) and the actuator fault (battery input current actuator). The TS fuzzy model is adopted for fuzzy modeling of the system and establishing fuzzy state observers. The concept of PDC (Kamal et al., 2017b) is employed to design fuzzy control and fuzzy adaptive observer from the TS fuzzy models. Sufficient conditions are derived for robust stabilization in the sense of Lyapunov stability. The sufficient conditions are formulated in the format of LMI (Linear Matrix Inequalities).
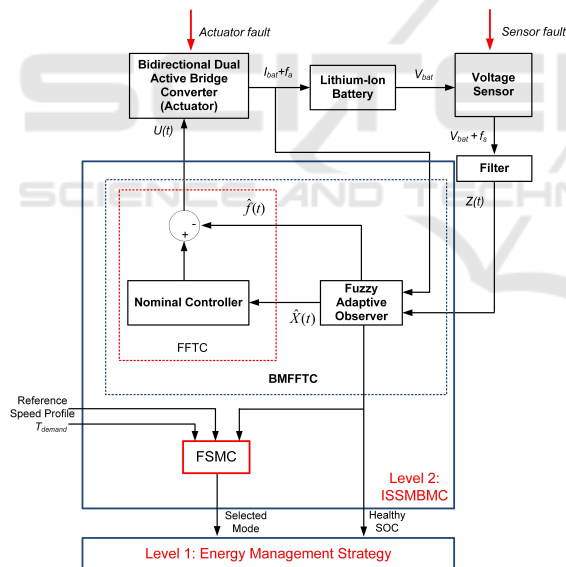
The general configuration of BMFFTC is shown in Figure 5, it is based on the fuzzy adaptive observer which estimates the sensor and actuator fault and reconstructs the controller. Fuzzy observer works with the Lithium-ion battery cell and based on the measured input current and output voltage, in order to battery state estimation. In this paper, the sensor fault or the actuator fault can occur at the same time or

only one sensor fault is present at a time. In order to design BMFFTC, we need to represent the battery model based on TS fuzzy model, design fault estimation based on the fuzzy adaptive observer as the following.

Takagi-Sugeno's Fuzzy Plant Model with Sensor and/or Actuator Faults. The overall fuzzy model achieved by fuzzy blending of each individual plant rule is given by (Kamal et al., 2012),

$$
\begin{aligned}
\dot{x}(t) &= \sum_{i=1}^{p} \mu_i(q(t))[A_i x(t) + B_i u(t) + E_{ai} f_a(t)] \\
y(t) &= \sum_{i=1}^{p} \mu_i(q(t))[C_i x(t) + E_{si} f_s(t)]
\end{aligned} \quad (5)
$$

where $x(t)$ is the state vector, $u(t)$ is the control input vector, $y(t)$ is the output vector, p is the number of rules of the TS fuzzy model, $A_i \in \kappa^{n \times n}$, $B_i \in \kappa^{n \times m}$ and $C_i \in \kappa^{g \times n}$ are system, input and output matrices, respectively and $q(t)$ are assumed measurable variables and do not depend on the sensor faults and the actuator faults. It is known that $\mu_i(q(t)) \geq 0$, $\sum_{i=1}^{p} \mu_i(q(t)) = 1$, writing $\mu_i(q(t))$ as μ_i for simplicity. Considering also the state $Z \in \kappa^{g \times 1}$ that is a filtered version of the output $y(t)$ (Edwards, 2006). This state is given by:

$$
\dot{Z}(t) = \sum_{i=1}^{p} \mu_i [-A_{zi} Z(t) + A_{zi} C_i x(t) + A_{zi} E_{si} f_s(t)] \quad (6)
$$

Where $-A_{zi} \kappa^{r \times r}$ is the stable matrix, from the (5) and (6), one can obtain the augmented system:

$$
\begin{aligned}
\dot{X}(t) &= \sum_{i=1}^{p} \mu_i [\bar{A}_i X(t) + \bar{B}_i U(t) + \bar{E}_i f(t)] \\
Y(t) &= \sum_{i=1}^{p} \mu_i \bar{C}_i X(t)
\end{aligned} \quad (7)
$$

where $X(t) = \begin{bmatrix} x(t) \\ Z(t) \end{bmatrix}$, $U(t) = \begin{bmatrix} u(t) \\ 0 \end{bmatrix}$, $f(t) = \begin{bmatrix} f_a(t) \\ f_s(t) \end{bmatrix}$, $\bar{A}_i = \begin{bmatrix} A_i & 0 \\ A_{zi} C_i & -A_{zi} \end{bmatrix}$, $\bar{B}_i = \begin{bmatrix} B_i & 0 \\ 0 & 0 \end{bmatrix}$, $\bar{E}_i = \begin{bmatrix} E_{ai} & 0 \\ 0 & A_{zi} E_{si} \end{bmatrix}$ and $\bar{C}_i = \begin{bmatrix} 0 \\ I \end{bmatrix}$, $A_i = \begin{bmatrix} \frac{1}{R_1 C_1} & 0 & 0 \\ 0 & \frac{1}{R_2 C_2} & 0 \\ 0 & 0 & 0 \end{bmatrix}$, $B_i = \begin{bmatrix} \frac{1}{C_1} \\ \frac{1}{C_2} \\ \frac{\eta}{C_n} \end{bmatrix}$,

Fuzzy Adaptive Observer. In order to estimate the state and the fault of the battery (4), the following fuzzy adaptive observer is proposed,

$$
\begin{aligned}
\dot{\hat{X}}(t) = \sum_{i=1}^{p} \mu_i [\bar{A}_i X(t) + \bar{B}_i U(t) \\
+ \hat{E}_i \hat{f}(t) + K_i (Y(t) - \hat{Y}(t))]
\end{aligned} \quad (8)
$$

$$
e_x(t) = X(t) - \hat{X}(t) + \hat{E}_i \hat{f}(t) + K_i(Y(t) - \hat{Y}(t))] \quad (9)
$$

$$
e_y(t) = Y(t) - \hat{Y}(t) = \bar{C}_i e_x(t) \quad (10)
$$

$$
\dot{\hat{f}}(t) = \sum_{i=1}^{p} \mu_i L_i (\dot{e}_y(t) + e_y(t)) = \sum_{i=1}^{p} \mu_i L_i \bar{C}_i (\dot{e}_x(t) + e_x(t)) \quad (11)
$$

$$
\hat{Y}(t) = \sum_{i=1}^{p} \mu_i \bar{C}_i \hat{X}(t) \quad (12)
$$

Where $\hat{X}(t)$ is the observer state, $\hat{Y}(t)$ is the observer output vector, $\hat{f}(t)$ is an estimation of the sensor and actuator fault $f(t)$, K_i and L_i are the observer gains to be designed. **Proposed Fuzzy Fault Tolerant Control.** In this section, the FFTC synthesis procedure is developed to deal with a wide range of sensor faults, and actuator faults while maintaining the stability of the closed loop battery system. For simplicity, we make $\bar{E}_j = \bar{B}_j E_j$, where, E_j are known matrix. For the fuzzy model (5), we construct the following FFTC via the PDC (Kamal et al., 2017b). It is assumed that the fuzzy system (5) is locally controllable. A state-feedback with LMIs is used to design a controller for each subsystem. The final output of the FFTC based on online fault estimation is defined by,

$$
U(t) = \sum_{j=1}^{p} \mu_j [G_j \hat{X}(t) - E_j \hat{f}(t)] \quad (13)
$$

where, G_i are the controller gain to be designed, the sensor and the actuator fault vectors are assumed to be bounded. The main result for the global asymptotic stability of a TS fuzzy model with sensor and actuator faults are summarized by the following Theorem 1.

Theorem 1: The TS fuzzy system (7) is asymptotically stabilizable if there exists symmetric and positive definite matrix P $(P>0)$, some matrices L_i, K_i, and G_j $(i=1,2,\ldots,p; j=1,2,\ldots,q)$, such that the following LMIs are satisfied,

$$
O A_i^T + A_i O - (B_i W_j)^T - (B_i W_j) < 0 \quad (14)
$$

$$
H_{bi}^T P_2 + P_2 H_{bi} - (D_i C_i)^T - (D_i C_i) < 0 \quad (15)
$$

where $O = P_1^{-1}$, $G_j = W_j O^{-1}$, $\bar{K}_i = P_2^{-1} D_i$, $\bar{K}_i = \begin{bmatrix} K_i \\ L_i \end{bmatrix}$.

Proof. The conditions imposed to develop the Theorem is shown in the appendix. According to the analysis above, the procedure for finding the proposed FFTC controller and the fuzzy adaptive observer for the battery are summarized as follows.

1. Obtain the mathematical model of the battery to be controlled (cf. section 2.3).

2. Obtain the TS fuzzy plant model for the system stated in the previous step by means of a fuzzy modeling method.

3. Solve LMIs (14) and (15) to obtain O, D_i, W_j, H_{bi}, P, L_i, K_i, and G_j thus ($O = P_1^{-1}$, $G_j = W_j O^{-1}$, $\bar{K}_i = P_2^{-1} D_i$, $\bar{K}_i = \begin{bmatrix} K_i \\ L_i \end{bmatrix}$).

4. Construct FFTC controller (13), fuzzy adaptive observer (8) to (12) according to the Theorem 1.

3.2 Energy Management Strategy (Level 1: EMS)

The design of this level is based on (Kamal et al., 2017a), this level of control manages and optimizes the power distribution between the two different sources based on new proposed formula to update the proposed fuzzy controller. Therefore, the mode of operation and healthy SOC set point are considered as two inputs for the second level of control (cf. Figure 5). There are six input variables at this control level: PCVE and actual vehicle torque for the learning adaptive algorithm and mode of operation with the same three inputs of the second level (speed of the vehicle, torque demand, SOC) for the fuzzy management controller. The two output variables of level 1 are $T_{ICE,SP}$ and $T_{EM,SP}$. The proposed fuzzy management controller inferred output for the ICE torque (T_{ICE}) and EM torque (T_{EM}) are given by (Kamal et al., 2017a),

$$T_{ICE} = \frac{\sum_{j=1}^{c} m_{ICE,j} \sigma_{ICE,j1} \sigma_{ICE,j2}}{\sum_{j=1}^{n} m_{ICE,j} \sigma_{ICE,j2}} \quad (16)$$

$$T_{EM} = \frac{\sum_{i=1}^{c} m_{EM,i} \sigma_{EM,i1} \sigma_{EM,i2}}{\sum_{i=1}^{c} m_{EM,i} \sigma_{EM,i2}} \quad (17)$$

where, $\sigma_{ICE,j1}$ and $\sigma_{EM,i1}$, $\sigma_{ICE,j2}$ and $\sigma_{EM,i2}$ are the mean and the standard deviation of the GMF of the output variable for the ICE and the EM, respectively, which are two adjustable parameter, $m_{ICE,j}$ and $m_{EM,i}$ are the inferred weights of the jth and i^{th} output membership function for the ICE and the EM, respectively, c is the number of fuzzy rules. The mean and the standard deviation of the output variable are optimize based on the proposed Learning Adaptive Algorithm (LAA) presented in the following section. In order to optimize the output of the proposed FMC based on Artificial Neural Network (ANN). We first identify the parameter sets involved in the premise and consequence control logic and use the proposed below Theorem 2 to updates the parameters values.

Theorem 2 (Kamal et al., 2017a): The parameters required by the FMC, shown in equations (16) and (17) are updated by the proposed LAA, if the mean and the standard deviation of the membership function satisfy the following:

$$\sigma_{ij1}^{k+1} = \sigma_{ij1}^{k} - \zeta^k \sum_{k=t+1}^{t+s} \sum_{j=1}^{N} \left(e_{ed}^k \mu_{td,ij} + e_{eff}^k \mu_{eff,ij} \right) \quad (18)$$

$$\sigma_{ij2}^{k+1} = \sigma_{ij2}^{k} - \zeta^k \sum_{k=t+1}^{t+s} \sum_{j=1}^{N} \left(e_{ed}^k \mu_{td,ij} + e_{eff}^k \mu_{eff,ij} \right) \quad (19)$$

where, σ_{ij1} is $\sigma_{ICE,j1}$ and $\sigma_{EM,i1}$ for (16) and (17), and σ_{ij2} is $\sigma_{ICE,j2}$ and $\sigma_{EM,i2}$ for (16) and (17) which are the mean and the standard deviation of the GMF for ICE and the EM, respectively. e_{td} and e_{eff} are the error functions for the torque demand and the vehicle total efficiency. $\mu_{td,ij}$ and $\mu_{eff,ij}$ are the weights of the ith rule for the jth training pattern, ζ^k is the learning rate, k is the iteration index, t is the trailing edge of the moving time-window over which the prediction error is minimized and s is the window of learning. For off-line learning we select $t = 1$ and $s = P$; where P is the size of the training set, which is usually much larger than the largest multi-step-ahead prediction horizon needed in practice (Gupta, 2015). The prediction accuracy deteriorates very quickly with increasing P. For on-line learning, s can be selected to be sufficiently large so as to include the largest possible prediction horizon (Gupta, 2015).

4 SIMULATION RESULTS AND DISCUSSION

To verify the BUSINOVA bus model and the control performance of the proposed overall control and optimal energy management strategy, simulation results under European driving cycle and variable road slope are presented. In order to develop and to evaluate the performance of the proposed overall energy management strategy (called REMS (cf. section 3)), a realistic model of the studied Hydraulic-Electric Hybrid bus included an accurate battery model is used (cf. Section 2) and implemented. In this section, three simulations and discussions to demonstrate the effectiveness of the proposed REMS are presented. The first simulation validatse the battery model at low and high temperature during discharging and the charging. In the second simulation, the effectiveness of the proposed strategy to detect and compensate the effect of battery fault and its effect on the SOC estimation are presented. The third simulation validates the overall control architecture for complete vehicle for Urban Dynamometer Driving Schedule (UDDS) to illustrate the effectiveness of the proposed technique.

4.1 Simulation 1: BUSINOVA Battery Model Validation

The objective of this section is to validate BUSI-NOVA bus battery model through experimental tests before implementing the diagnostic scheme. BUSI-NOVA bus battery cell has rated capacity of 80 Ah and nominal voltage of 4.1 V. The simulations have been performed using the equivalent circuit-based model provided in section 2.3. The proposed strategy will validate in two cases using real data in high temperature region and low temperature region for discharging and charging. Figure 6 (left) shows the for the discharging current profile. Figure 7 shows the comparison of experimental and model output voltage and the voltage error for discharging at low temperature -40^oC. Figure 8 shows the comparison output voltage and the voltage error for charging at thigh temperature 40^oC for the pulsating current given in Figure 6 (right).
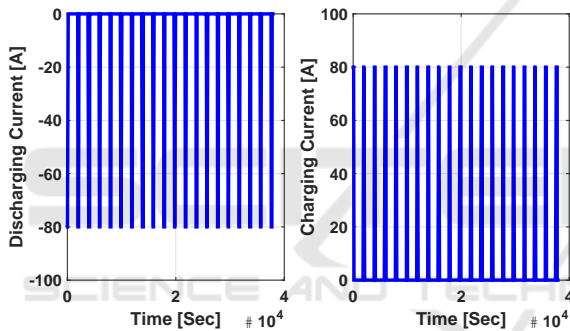
Figure 6: Battery current profile; (left) battery discharging current profile; (right) battery charging current profile.

From Figures 7 and 8, one can observe that the proposed model of Lithium-ion battery gives an accurate modeling performance despite the system nonlinearities, temperature and SOC variation. For the proposed model, between 0% and 100% SOC, the standard deviation of voltage has mean value error of ∼0.5 mV, or ∼0.2% of the operating voltage range at different temperature and current (80A), which is less error compared terminal voltage error of 1.5% (Sepasi et al., 2014).

4.2 Simulation 2: Fault Detection and its Effects on Battery SOC Estimation

The objective of BMFFTC for the Lithium-ion battery presented in section 3.1.2 is to ensure that all signals in the closed-loop battery system are bounded during the battery faults. In this section, the effects of current
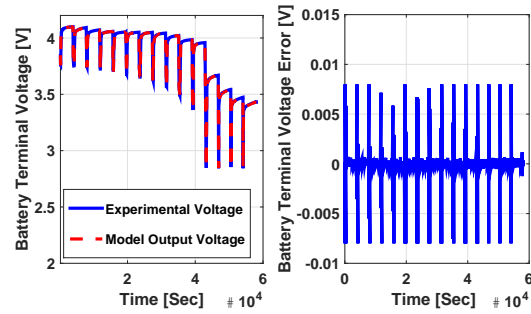

Figure 7: Comparison of experimental and model output voltages and voltage error for discharge at -40^oC and 80A; (left) experimental and model output voltages; (right) voltage error.
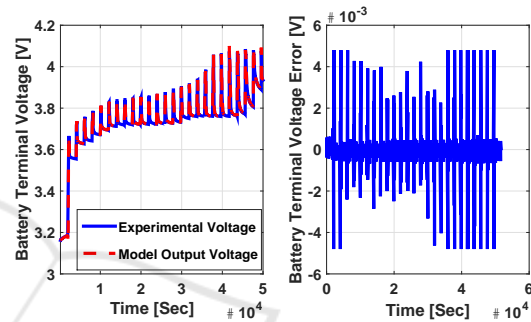

Figure 8: Comparison of experimental and model output voltages and voltage error for charge at 40^oC and 80A; (left) experimental and model output voltages; (right) voltage error.

or voltage sensor faults on the battery SOC estimations and compensate its effect are investigated.The advantage of the proposed strategy can detect and estimates time varying or/and constant fault. For the testing purpose, it is required that sensor and/or actuator fail. The current or voltage sensor faults are injected in the battery test bench. The initial value of the fuzzy observer SOC state is 50%. The tested discharging current profile is given in Figure 9. Figure 10 (left) and (right) show the current sensor fault (+20 A bias fault) and voltage sensor fault (+0.1 V bias fault) (solid lines) and their estimations (dashed lines) based on the fuzzy observer, respectively. To prevent the battery from over-discharge, the lower limit of the battery SOC is taken as 10%. We are considered the ±20 A bias sensor fault occur at the time 2406 sec. Figure 11 (left) plots the experimental SOC estimation under the current sensor fault with FFTC and without FFTC, while Figure 11 (right) shows the SOC estimation errors. It can be found from Figure 11 (left) that the computed SOC in battery management system (observer-estimated SOC) is around 20% at the time 4812 sec when the current sensor has a +20 A bias fault. According to this result, the battery suffering from over-discharge. Therefore, this will accel-

erate the battery aging and decrease the battery life. For a -20 A bias fault, the estimated SOC will reach to 10% and the battery cannot release the supposed energy. Also with ±0.1 V bias fault at the time of 2406 sec, similar simulation results are obtained in Figure 12 (left) and (right). The battery may be over-discharged when the voltage sensor has a $+0.1$ V fault as shown in Figure 12 (left). The estimation errors are up to 22% with the voltage sensor faulty condition (cf. Figure12 (right)). The results show that the battery may be over-discharged in the faulty sensor cases. The simulation results demonstrate the effectiveness of the proposed control approach. The proposed control scheme can guarantee the stability of the closed-loop battery system.

4.3 Simulation 3: Proposed Overall Strategy Validation

The purpose of this section is to validate the proposed overall control architecture for optimal energy management. The proposed scheme is experimentally tested under the UDDS (Urban Dynamometer Driving Schedule) and test conditions, including the recorded faulty current or voltage data at room temperature. Figures 13 and 14 depict the trajectories of bus velocity, and the torque under the UDDS drive cycle, respectively. It is seen that the output speed and torque of the vehicle is similar to the reference speed profile and the torque demand of this drive cycle. The final goal of the proposed strategy is to minimize the total energy consumption of the vehicle even during the battery faults over the complete drive cycle, permitting thus to increase the efficiency and the robustness of the vehicle energy management strategy. The battery SOC for the studied driving cycle UDDS is given in Figure 15. Figure 16 shows the total energy consumption by the vehicle during the UDDS complete cycle. From the simulation results, it is found that the proposed strategy can be applied to the power assignment for studied HHEV even if the future driving cycle is unknown because it does not require beforehand a-priori knowledge of the driving events.

From the simulation results, it can be seen that without the reconfiguration mechanism, the battery lost performance just after the sensor became faulty, whereas for the same condition and using the proposed FFTC scheme strategy, the battery remains stable in the presence of voltage sensor fault and current actuator fault which demonstrates the effectiveness of the proposed FFTC strategy.

In summary, it can be seen that the BUSINOVA bus follows the trajectory of the reference input. Thus, if driving cycles are changed, the control effect
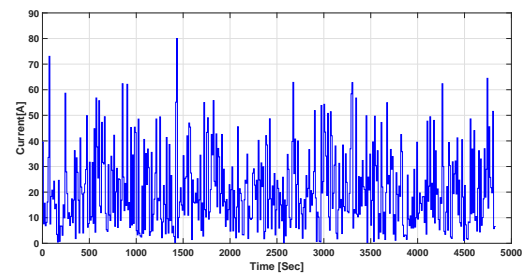

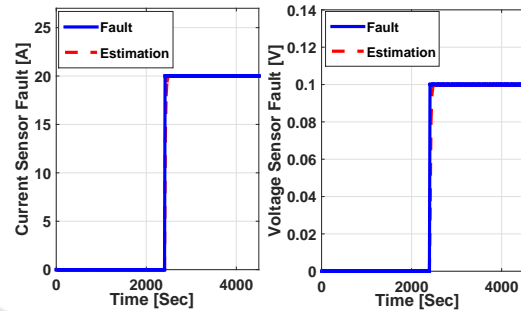
Figure 9: Battery discharging current profile.

Figure 10: Battery current and voltage sensor faults and their estimations; (left) battery current sensor fault and its estimation; (right) battery voltage sensor fault and its estimation.
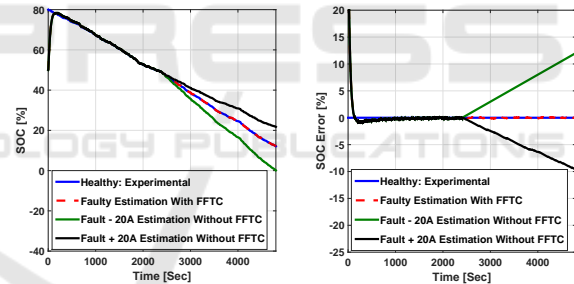

Figure 11: Effects of current fault on battery SOC estimation; (left) SOC estimation results in the current sensor faulty conditions with FFTC and without FFTC; (right) SOC estimation errors in the current sensor faulty conditions with FFTC and without FFTC.

of the proposed strategy remains as accurate as the results under UDDS cycle. In addition, the proposed overall control architecture for optimal energy management is reliable even during current and/or voltage sensor faults (cf. Section 4.2).

5 CONCLUSION

This paper presented a robust energy management strategy, with battery faults detection and compensation for the studied hydraulic-electric hybrid vehicle. In the first part, an appropriate design of systematic
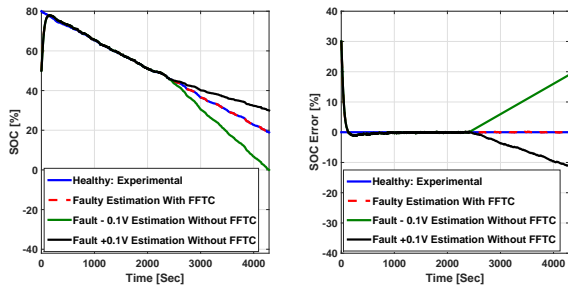
Figure 12: Effects of voltage fault on battery SOC estimation; (left) SOC estimation results in the voltage sensor faulty conditions with FFTC and without FFTC; (right) SOC estimation errors in the voltage sensor faulty conditions with FFTC and without FFTC.
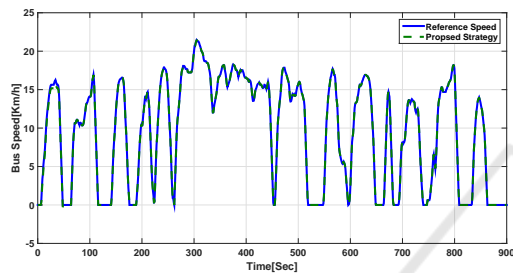

Figure 13: Comparisons between reference speed and actual vehicle speed [Km/h] for proposed strategy over UDDS cycle.
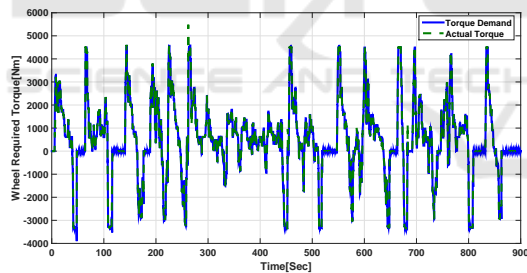

Figure 14: Comparisons between reference torque and actual vehicle torque [Nm] for proposed strategy over UDDS cycle.

BMFFTC (Battery Management Fuzzy Fault Tolerant Controller) scheme is proposed to estimate and compensate the battery faults. Some sufficient conditions for robust stabilization of the TS fuzzy model were derived for a Lithium-ion battery and were formulated in an LMI (Linear Matrix Inequalities) format. The second part of the paper has been focused on minimizing total energy consumption and thereby on increasing the total distance traversed between refueling of the studied hybrid vehicle. The proposed method has been implemented using real time power management strategy, named Robust Energy Management Strategy (REMS). This proposed strategy consists of two control levels. The highest one (the second level) has
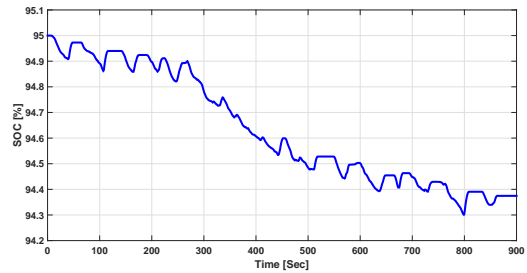

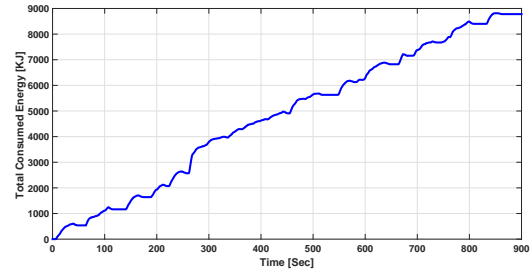Figure 15: SOC for the proposed strategy over UDDS cycle.

Figure 16: Total energy consumed by the vehicle [KJ] for proposed strategy over UDDS cycle.

been developed using fuzzy strategy and fuzzy observer in order: to manage all of the possible bus operation modes, generates SOC set point for second level and compensate the battery faults. At the first level, an energy management strategy has been developed for power splitting which decides the optimal combination of power sharing (between different energy sources) to minimize the total bus energy consumption while maximizing the overall vehicle efficiency. The obtained results confirm that, using the proposed approach: (i) the strategy can be easily implemented in real time because it does not depend on prior information about future driving conditions; (ii) battery faults could be accurately detected and compensated to minimize its aging effects; (iii) minimize total energy consumption; (iv) mean and the standard deviation of the membership function of the fuzzy logic controller are optimized based on neural-network. It is planned in near future to implement the overall proposed control strategy on the actual BUSINOVA platform.

ACKNOWLEDGEMENTS

REFERENCES

Abdrakhmanov, R. and Adouane, L. (2017). Efficient acc with stopgo maneuvers for hybrid vehicle with online sub-optimal energy management. In *11th International Workshop on Robot Motion and Control, Wasowo-Poland, 3-5 July*. RoMoCo'17.

Edwards, C. (2006). A comparison of sliding mode and unknown input observers for fault reconstruction. In *vol.12, no.3, pp. 245-260*. European journal of control.

Gupta, V. (2015). Optimization trilogy for energy management in parallel hybrid electric vehicles. In *vol. 17, pp.1-12*. HCTL Open International Journal of Technology Innovations and Research (IJTIR).

Hamed, B. and Almobaied, M. (2011). Fuzzy pid controllers using fpga technique for real time dc motor speed control. In *vol. 2, pp. 233-240*. Intelligent Control and Automation.

Hou, C., Ouyang, M., Xu, L., and Wangi, H. (2014). Approximate pontryagin's minimum principle applied to the energy management of plug-in hybrid electric vehicles. In *vol. 115, pp. 174-189*. Applied Energy.

Kamal, E., Adouane, L., Abdrakhmanov, R., and Ouddah, N. (2017a). Hierarchical and adaptive neuro-fuzzy control for intelligent energy management in hybrid electric vehicles. In *World Congress, 9-14 July, Toulouse-France*. IFAC.

Kamal, E., Adouane, L., Aitouche, A., and Mohammed, W. (2017b). Robust power management control for stand-alone hybrid power generation system. In *vol. 783, pp. 12-25*. Journal of Physics: Conference Series.

Kamal, E., Aitouche, A., Ghorbani, R., and Bayart, M. (2012). Robust fuzzy fault tolerant control of wind energy conversion systems subject to sensor faults. In *Transactions on Sustainable Energy, vol. 3, no 2, pp. 231-241*. IEEE.

Lu, L., Han, X., Li, J., Hua, J., and Ouyang, M. (2013). A review on the key issues for lithium-ion battery management in electric vehicles. In *vol. 226, pp. 272-288*. J. Power Sources.

Maleki, H. and Howard, J. N. (2006). Effects of overdischarge on performance and thermal stability of a li-ion cell. In *vol. 160, no. 2, pp. 1395-402*. J. Power Sources.

Martnez, C. M., Hu, X., Cao, D., Velenis, E., Gao, B., and Weller, M. (2016). Energy management in plug-in hybrid electric vehicles: Recent progress and a connected vehicles perspective. In *Transactions on Vehicular Technology, vol. PP, no.99, pp.1-16*. IEEE.

Panday, A. and Bansal, H. O. (2016). Energy management strategy implementation for hybrid electric vehicles using genetic algorithm tuned pontryagin's minimum principle controller. In *vol. 2016, pp.1-13*. International Journal of Vehicular Technology.

Plett, G. L. (2004). Extended kalman filtering for battery management systems of lipb-based hev battery packspart 3. state and parameter estimation. In *vol. 134, pp. 277-29*. J. Power Sources.

Sepasi, S., Ghorbani, R., and Liaw, B. Y. (2014). A novel on-board state-of-charge estimation method for aged lithium-ion batteries based on model adaptive extended kalman filter. In *vol. 245, pp.337-344*. J. Power Sources.

Striebel, K., Shim, J., Sierra, A., Yang, H., Song, X., Kostecki, R., and McCarthy, K. (2005). The development of low cost lifepo4-based high power lithium-ion batteries. In *vol.146, pp. 33-38*. J. Power Sources.

Tate, E., Grizzle, J., and Peng, H. (2010). Sp-sdp for fuel consumption and tailpipe emissions minimization in an evt hybrid. In *Transactions on Control Systems Technology,vol. 18, no. 3, pp. 673-687*. IEEE.

Tulpule, P., Marano, V., and Rizzoni, G. (2010). Energy managemernt for plug-in hybrid electric vehicles using equivalent consumption minimisation strategy. In *vol. 2 , no.4, pp. 329-350*. Int J. Electric and Hybrid Vehicles.

Xing, Y., Ma, E. W. M., Tsui, K.-L., and Pecht, M. (2013). An ensemble model for predicting the remaining useful performance of lithium-ion batteries. In *vol. 53, no. 6, pp. 811-820*. Microelectronics Reliability.

APPENDIX

This appendix gives the proof for the Theorem 1. In order to carry out the analysis for BMFTC, the closed-loop fuzzy system should be obtained first by establishing the conditions for the asymptotic convergence of the observers. The fuzzy control system of the state and the errors can be obtained. Substituting (13) into (7) and (8), we obtain the dynamics of the closed loop system and the state estimation error.

Therfore, from (9), (10), (11) and (12), we obtain

$$
\begin{aligned}
\dot{X}(t) = &\sum_{i=1}^{p}\sum_{j=1}^{p} \mu_i\mu_j[(\bar{A}_i + \bar{B}_i\,G_j)X(t) + \bar{E}_i f(t)] \\
&- \sum_{i=1}^{p}\sum_{j=1}^{p}\mu_i\mu_j\bar{B}_i\,G_j e_x(t) - \sum_{i=1}^{p}\mu_j\bar{B}_iE_i\hat{f}(t)]
\end{aligned} \tag{20}
$$

Let

$$
\tilde{f}(t) = f(t) - \hat{f}(t) \tag{21}
$$

From(20) and (21), a TS fuzzy closed-loop can be observed:

$$
\begin{aligned}
\dot{X}(t) = &\sum_{i=1}^{p}\sum_{j=1}^{p} \mu_i\mu_j[(\bar{A}_i + \bar{B}_i\,G_j)X(t) \\
&- \bar{B}_i\,G_j\,e_x(t) + \bar{E}_i\tilde{f}(t)]
\end{aligned} \tag{22}
$$

Then taking the derivative of $e_x(t)$ in (9) and substituting from (7), (8) and (21), the following is obtained:

$$
\dot{e}_x(t) = \sum_{i=1}^{p}[(\bar{A}_i - K_i\bar{C}_i)e_x(t) + \bar{E}_i\tilde{f}(t)] \tag{23}
$$

The derivative of $\tilde{f}(t)$ in (21) can be written as,

$$
\begin{aligned}
\dot{\tilde{f}}(t) = &\dot{f}(t) - \dot{\hat{f}}(t) = \dot{f}(t) - \sum_{i=1}^{p}\mu_i L_i\bar{C}_i \\
&(\sum_{i=1}^{p}[(\bar{A}_i - K_i\bar{C}_i + I)e_x(t) + \bar{E}_i\tilde{f}(t)])
\end{aligned} \tag{24}
$$

Combining (22), (23) and (24) yields the following augmented fuzzy system.

$$
\begin{aligned}
\dot{\tilde{X}}(t) &= \sum_{i=1}^{p} \mu_i \mu_j [\tilde{H}_{ij} \tilde{X}(t) + \tilde{E}_i F(t)] \\
\tilde{Y}(t) &= \sum_{i=1}^{p} \mu_i \tilde{C}_i \tilde{X}(t)
\end{aligned}
\qquad (25)
$$

with $\tilde{X}(t) = \begin{bmatrix} X(t) \\ e_x(t) \\ \tilde{f}(t) \end{bmatrix}$, $F(t) = \begin{bmatrix} 0 \\ 0 \\ \dot{f}(t) \end{bmatrix}$,

$\tilde{H}_{ij} = \begin{bmatrix} (\bar{A}_i + \bar{B}_i G_j) & H_{1ij} \\ 0_{2x1} & H_{2ij} - \bar{K}_i \bar{C}_{1i} \end{bmatrix}$, $\bar{K}_i = \begin{bmatrix} K_i \\ L_i \end{bmatrix}$,

$H_{1ij} = \begin{bmatrix} -\bar{B}_i G_j & \bar{E}_i \end{bmatrix}$, $\tilde{C}_i = \begin{bmatrix} \bar{C}_i \\ 0 \end{bmatrix}^T$, $\tilde{E}_i = \begin{bmatrix} 0 & 0 \\ 0 & I \end{bmatrix}$,

$H_{2ij} = \begin{bmatrix} \bar{A}_i & \bar{E}_i \\ -L_i \bar{C}_i (\bar{A}_i - K_i \bar{C}_i) & -L_i \bar{C}_i \bar{E}_i \end{bmatrix}$.

Let us consider the following quadratic Lyapunov candidate function $V(t)$:

$$
V(t) = \tilde{X}(t)^T P \tilde{X}(t) \qquad (26)
$$

where P is common positive definite matrix. The problem of robust state and fault estimation is to find the gains G_j, K_i and L_i of the controller and the observers to ensure an asymptotic convergence of $X(t)$ toward zero when $F(t) = 0$. This problem is reduced to find P verifying $V(t) < 0$, i.e.,

$$
\dot{\tilde{X}}(t) = \sum_{i=1}^{p} \mu_i \tilde{H}_i \tilde{X}(t) \qquad (27)
$$

The derivative time of $V(t)$ is given by

$$
\dot{V}(t) = \frac{1}{2} \dot{\tilde{X}}(t)^T P \tilde{X}(t) + \frac{1}{2} \tilde{X}(t)^T P \dot{\tilde{X}}(t) \qquad (28)
$$

By substituting (27) into (28), one obtain

$$
\dot{V}(t) = \frac{1}{2} \tilde{X}(t)^T \sum_{i=1}^{p} \mu_i (\tilde{H}_i^T P + P \tilde{H}_i \tilde{X})(t) \qquad (29)
$$

From (29), the derivative time of (26) is uniformly negative if the following inequality is satisfied

$$
P \tilde{H}_{ij} + \tilde{H}_{ij}{}^T P < 0 \qquad \forall i, j \qquad (30)
$$

Let $P = \begin{bmatrix} P_1 & 0 \\ 0 & P_2 \end{bmatrix}$, Therefore, the inequality (30) will be rewritten as:

$$
P_1 (A_i - B_i G_j) + (A_i - B_i G_j)^T P_1 < 0 \quad \forall i, j \qquad (31)
$$

$$
P_2 (H_{bi} - \bar{K}_i \bar{C}_i) + (H_{bi} - \bar{K}_i \bar{C}_i)^T P_2 < 0 \quad \forall i, j \qquad (32)
$$

By multiplying(31) from left and right by $O = P_1^{-1}$, and applying the change of variables $O = P_1^{-1}$, $W_j = G_j O$, $D_i = P_2 \bar{K}_i$, LMIs (14) and (15) are obtained.